JCTC Journal of Chemical Theory and Computation

ARTICLE

pubs.acs.org/JCTC

Structural Instability of the Active Site of T1 Lipase Induced by Replacement of Na^+ with Water Complexed with the Phenylalanine Aromatic Ring

Yohsuke Hagiwara,[†] Jiyoung Kang,[†] and Masaru Tateno*[,‡]

[†]Graduate School of Pure and Applied Sciences, University of Tsukuba, 1-1-1 Tennodai, Tsukuba Science City, Ibaraki 305-8571, Japan

[‡]Graduate School of Life Science, University of Hyogo, 3-2-1 Kouto, Kamigohri, Akoh, Hyogo 678-1297, Japan

Supporting Information

ABSTRACT: The crystallographic analysis of T1 lipase suggested an interaction between Na^+ and the aromatic ring of Phe16 in the active site. However, experimental approaches could not dismiss the possible presence of water instead of Na^+. Our previous molecular dynamics (MD) simulations suggested that the significantly large enthalpy gain of the $Na^+-\pi$ interaction was required to preserve the catalytic core structure of T1 lipase. In this study, to examine the effects of water, we performed further MD simulations of T1 lipase involving the water$-\pi$ interaction, instead of the $Na^+-\pi$ interaction, exploiting various force fields, such as ff99, ff02, and an accurate potential field to describe the water$-\pi$ interaction, which was generated using our recently developed scheme (referred to as the grid-based energy representation). The analyses revealed that the water$-\pi$ complex was unstable in the catalytic core of T1 lipase even when the accurate potential of the water$-\pi$ complex represented by the grid-based energy function was employed in the MD simulations and led to the disruption of the coordinated structure. In contrast, the catalytic core structure of T1 lipase involving the $Na^+-\pi$ complex was significantly stable in the 10 ns MD simulation using the grid-based energy representation of the $Na^+-\pi$ interaction. Thus, the possible presence of water may be excluded, and our previous proposal concerning the functional role of the structural element involving the $Na^+-\pi$ interaction in the catalytic site of T1 lipase has unambiguously been confirmed. Further, the strong coordination of Na^+ and N_ε of His358 was also shown to be substantial to preserve the core structure of the catalytic site.

1. INTRODUCTION

The cation$-\pi$ interaction is a noncovalent binding interaction, in which a cation is strongly attracted to the π electrons of an aromatic molecule. The interaction is commonly found in biological macromolecules and contributes to their structural stability and to drug−protein interactions.[1−6] Even though only about 10 years have passed since such functional roles were proposed, cation$-\pi$ interactions are now recognized as being as important as other conventional noncovalent interactions, i.e., hydrogen bonds, salt bridges, and hydrophobic interactions. The cations participating in the interactions include metal cations, such as Na^+ and Mg^{2+}, which are abundant in living organisms, as well as positively charged amino acid residues, including arginine (Arg) and lysine (Lys). Substantial stabilization energy has been detected in the gas phase[7−12] and also in aqueous solutions[2,13−15] upon the formation of metal$-\pi$ interactions. However, only a few experimental structures containing complexes of metal cations and aromatic rings have been reported.[16−20] Thus, the functional roles of the interactions remain to be clarified.

The X-ray crystallographic analysis of a thermoalkalophilic lipase from *Geobacillus zalihae* strain T1 (T1 lipase) revealed a characteristic feature; i.e., a spherical electron density was detected in the vicinity of the Phe16 side chain in the catalytic site (Figure 1).[21] Since T1 lipase exhibits its catalytic activity under alkaline physiological conditions, which provide an abundance of Na^+ ions, such as in palm oil mill effluent (POME),[22] the electron density was considered to correspond to Na^+. However, the possibility that the electron density corresponded to a water molecule, rather than Na^+, could not be ruled out.[21] Actually, a survey of a set of 75 high resolution crystal structures of proteins (less than 1.1 Å) revealed the existence of such water$-\pi$ interactions, and 18 water molecules were found facing the planes of the aromatic rings.[23]

In our previous study, to investigate whether the electron density actually corresponds to Na^+, we performed molecular dynamics (MD) simulations of T1 lipase, where Na^+ was placed at the active site.[24] However, conventional force fields occasionally fail to provide an accurate description of the metal$-\pi$ interactions. Accordingly, we developed a novel strategy, the "grid-based energy representation" scheme, which enables us to calculate their interaction energy with an accuracy corresponding to that of advanced *ab initio* post Hartree−Fock methods and a computational cost comparable to that of force field calculations.[24] A comparison of the MD simulation results obtained using the grid-based energy representation with those generated using the conventional force fields (polarizable and nonpolarizable ones) showed that an accurate estimation of the large binding energy (approximately 20 kcal/mol) was essential to correctly reproduce the experimental structure of the catalytic core of T1 lipase. In other words, a smaller interaction energy (∼10 kcal/mol, estimated by the nonpolarizable force field, AMBER ff99[25]) caused serious structural disruptions.

Received: December 26, 2010
Published: June 14, 2011

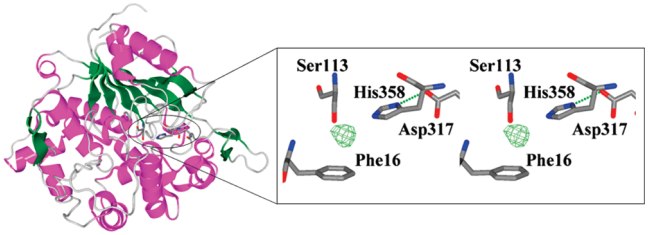

Figure 1. Crystal structure of the *Geobacillus zalihae* T1 lipase (PDB code: 2DSN). A close-up view of the configuration of the catalytic site is also shown in the right panel (stereo view). In the active site, a spherical electron density is observed, and the corresponding molecule is coordinated to the side chains of Phe16, Ser113, and His358.

Table 1. Summary of the MD Simulations Conducted in This Study

identify of the spherical electron density	H_2O			Na^+
potential field	ff99	ff02	GER[a]	GER[a]
single-protonated His358	5 ns	5 ns	5 ns	10 ns[b]
double-protonated His358	5 ns	5 ns	10 ns	–[c]

[a] The grid-based energy representation (GER) was exploited. [b] In our previous study, a 5 ns MD simulation was performed;[24] in the present study, this MD simulation was extended up to 10 ns to confirm the structural convergence. [c] Not performed.

This excluded the possibility of the presence of water in the catalytic core, since the energy gain of the water–π interaction is ~4 kcal/mol.[26] Moreover, we have proposed the functional roles of the Na^+–Phe16 interaction; i.e., it establishes a remarkably stable core structure by combining a hydrophobic aromatic ring (Phe16) and hydrophilic residues (Ser113 and His358), with the latter forming the catalytic triad. It was also implied that the rigid core structure formed by the Na^+–π interaction may contribute to the large structural changes from the complex with ligands to the free form of the enzyme.

In the present study, to clarify the identity of the electron density, i.e., water or Na^+, we performed additional MD simulations in which a water molecule was, in turn, assigned to the electron density (all of the MD simulations conducted in this study are summarized in Table 1). Since our previous study demonstrated the importance of an accurate description of the interaction energy,[24] in the present study, we also evaluated the feasibility of the conventional force fields, i.e., ff99 and ff02,[27] for the estimation of the water–π interaction energy and confirmed the poor accuracy of the force fields. Accordingly, we applied our grid-based energy representation scheme to conduct the MD simulation, which included the potential function for the accurate estimation of the interaction energy. The results of the MD simulation showed the serious instability of the water–Phe16 complex, leading to the structural disruption of the complex. These results provide further evidence that Na^+, rather than water, is bound to Phe16 in the active site of T1 lipase.

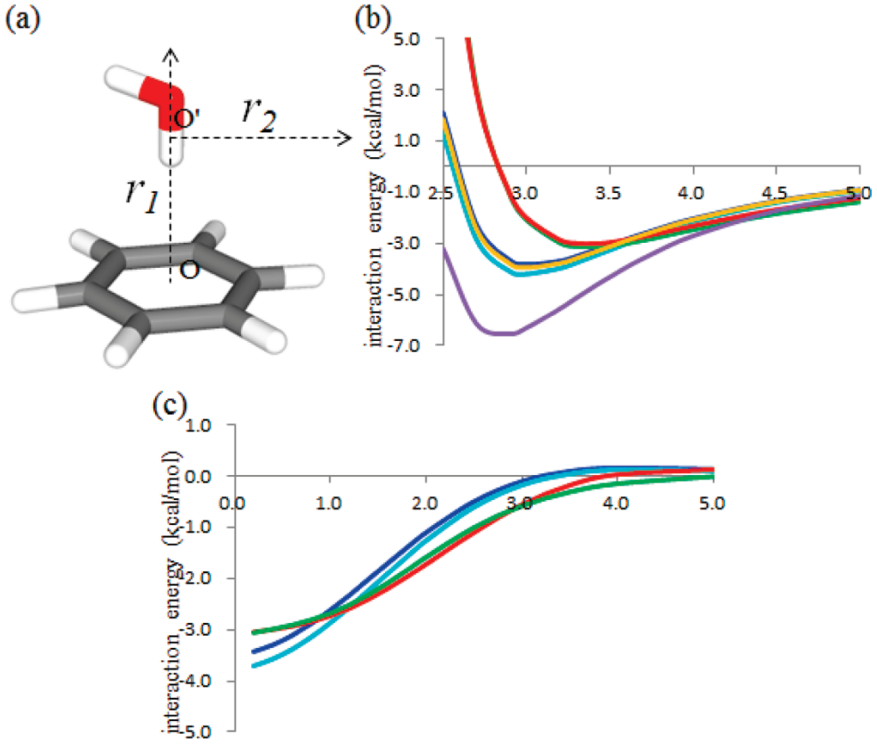

Figure 2. (a) Model structures for water–π interactions, where the oxygen atom of the water is placed on a line perpendicular to the benzene ring and passing through the center of mass of the benzene ring O. r_1 denotes the distance of the oxygen atom from O. O′ is the point where r_1 is 3.3 Å (which is the optimal distance of r_1 in the potential curve), and r_2 denotes the distance of the oxygen atom from O′ along a line parallel to the benzene ring and passing through O′. Energy profiles of the interaction energies of the water and the benzene ring with respect to (b) r_1 and (c) r_2. The interaction energies of the water–benzene system obtained by MP2/aug-cc-pvtz and the molecular mechanics calculations using ff99 and ff02 are shown in red, blue, and light blue, respectively. The interaction energies obtained by ff02, in which the parameters responsible for the polarization are increased 8-fold (purple) and decreased 0.3-fold (orange) with respect to the original parameter values, to describe the polarizability. The energy potential curves obtained by the grid-energy representation are shown in green.

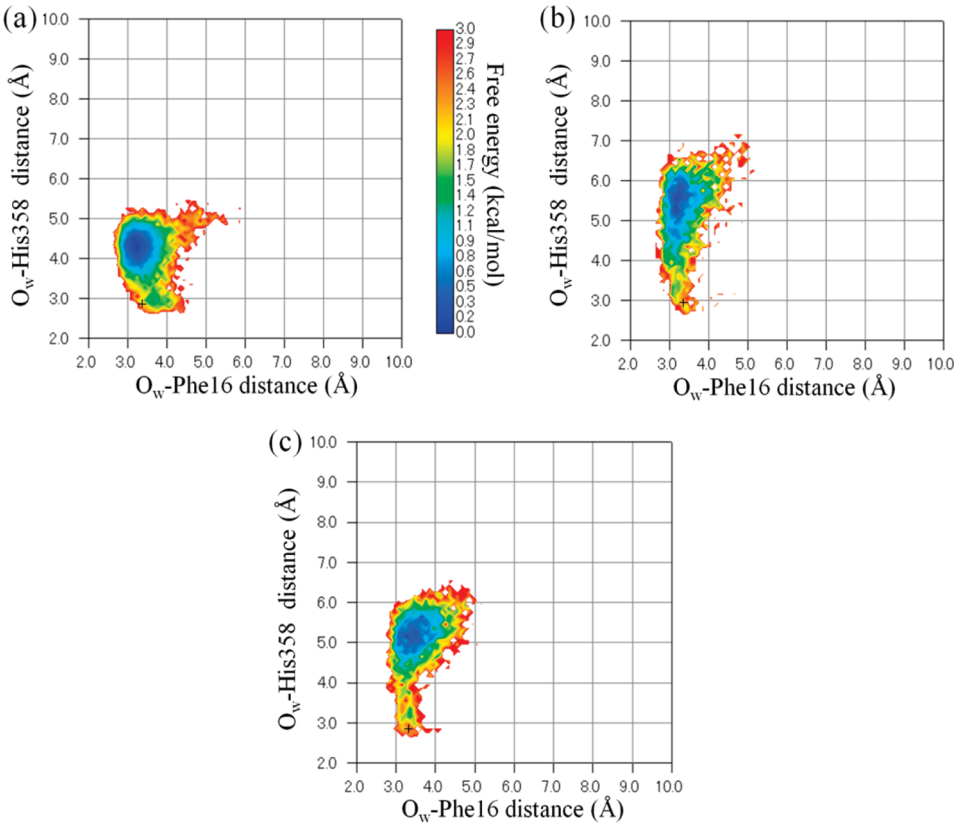

Figure 3. Free energy landscapes obtained by standard MD simulations (5 ns) of T1 lipase using ff99 (a), ff02 (b), and the grid-based energy representation (c). The vertical axis shows the distance between the oxygen atom of the water molecule (O_w) and N_ε of His358, and the horizontal axis is the distance between the oxygen atom and the center of mass of the Phe16 side chain. A cross (+) represents the crystal structure.

RESULTS AND DISCUSSION

Evaluation of Force Fields. First, we evaluated the feasibility of a nonpolarizable force field, ff99, and a polarizable force field, ff02, for the estimation of the interaction between a water molecule and an aromatic ring, benzene. For the calculations, we constructed model structures in which a hydrogen atom of the water was pointed toward the benzene (Figure 2a). The interaction that generates the binding force in such a conformation is referred to as an OH$-\pi$ interaction, which is a hydrogen bond where the π electrons of the aromatic ring act as the hydrogen bond acceptor.[23]

Then, we calculated the potential curves with respect to the distance between the oxygen atom of the water and the center of mass of the benzene, using three methodologies, ff99, ff02, and MP2/aug-cc-pvtz (Figure 2b). In this study, MP2 was employed to obtain the reference values; the correction of the MP2 results to estimate values calculated using the coupled-cluster with singles, doubles, and perturbative triples (CCSD(T)), as conducted in our previous study,[24] would not be required in this case for the following reason: The water$-\pi$ interaction is dominated by a hydrogen bond property that is accurately described by MP2,[26,28,29] whereas the correction is essential for the evaluation of the $\pi-\pi$ interaction, which MP2 significantly overestimates. In fact, the MP2 results have been used as the reference in other recent studies.[30−32]

According to the potential curve calculated using MP2, the energy minimum is located at 3.3 Å, where the stabilization energy is 3.11 kcal/mol. On the other hand, the energy minima in the potential curves calculated using ff99 and ff02 are located at 3.0 Å in both cases, and the minimum energies were found to be overestimated by 0.71 and 1.08 kcal/mol, respectively. To consider other configurations, we constructed model structures in which the oxygen atom was placed on the axis that is parallel to the aromatic ring (Figure 2a). In the figure, O′ denotes the cross point of the two axes (r_1 is 3.3 Å), and r_2 is defined as the distance between the oxygen atom and O′. With respect to the second configuration, the conventional force fields overestimated the minimum energy, as observed in Figure 2c, whereas the stabilization energies at larger distances (r_2 > 1.0 Å) were underestimated.

In this manner, the conventional force fields are not consistent with the reference potential curve calculated using MP2/aug-cc-pvtz. However, we performed the molecular dynamics (MD) simulations of T1 lipase using those potential fields to evaluate the effects of the differences in the energy potentials, since this strategy was informative in our previous study. The initial structure of the protein was obtained from its crystal structure (Figure 1), but the Na^+ in its active site was replaced with a water molecule (the oxygen atom of the water was placed at the coordinates of the Na^+).

MD Simulation Using ff99. First, we examined ff99 in a 5 ns MD simulation. Using the resultant MD trajectory, we calculated the two-dimensional (2-D) free energy profile with respect to the distance between the oxygen atom of the water molecule and the center of mass of the aromatic ring of Phe16, and that between the oxygen atom and N_ε of His358 (Figure 3a). It showed that the minimum corresponds to a structure that is not observed in

the crystal structure. In particular, the inconsistency of the water−N_ε distance is remarkable, for the following reason: In the MD simulation, the N_ε of His358 is stably hydrogen-bonded with the hydrogen atom of the hydroxyl group of the Ser113 side chain (Figure 4a). This hydrogen bond prevents the water from forming the hydrogen bond with N_ε of His358, due to the steric clash between the hydrogen atoms of the water and the Ser113 side chain, which causes the increased water−N_ε distance (the reasons for the structural changes are further discussed later).

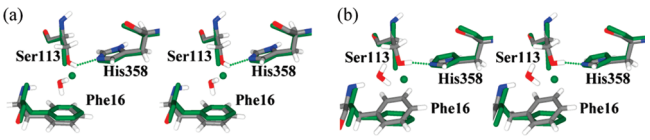

Figure 4. Conformations of the most stable state in Figure 3a (a) and Figure 3b (b). The crystal structure of the *Geobacillus zalihae* lipase is colored green. The green sphere represents the position of Na^+ in the crystal structure. The snapshots of the MD simulations are shown in atom-specific colors.

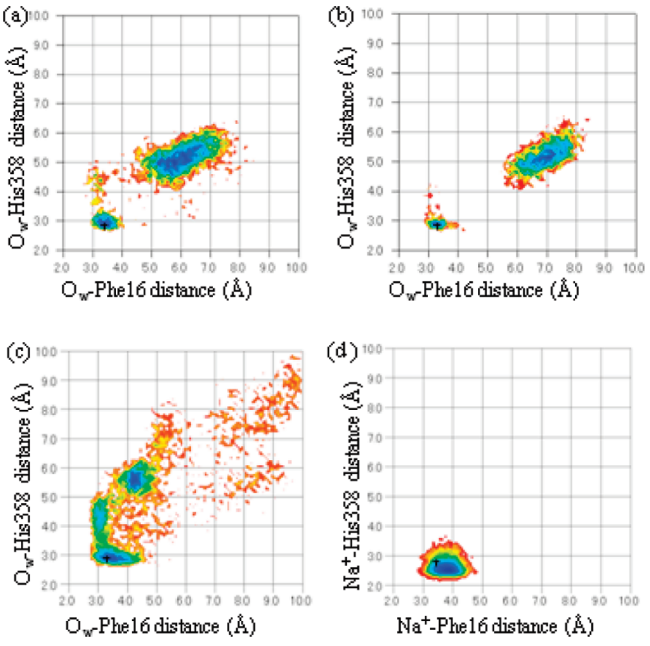

Figure 5. Free energy landscapes obtained by standard MD simulations of T1 lipase, in which the doubly protonated form is assigned to His358, using ff99 (5 ns) (a), ff02 (5 ns) (b), and the grid-based representation (10 ns) (c). The vertical axis shows the distance between the oxygen atom of the water molecule (O_w) and N_ε of His358, and the horizontal axis is the distance between the oxygen atom and the center of mass of the Phe16 side chain. The cross (+) represents the crystal structure. Panel (d) shows the free energy profile obtained with the 10 ns MD simulation where Na^+ was assigned to the electron density instead of a water, using the grid-based representation. In this calculation, the state of His358 is the single protonated form.

It should be noted here that Asp317 is coordinated to His358 (Figure 1); its pK_a value was calculated as 3.85 using PROPKA 2.0.[33] Due to the presence of this aspartate residue, His358 is considered to be in the singly protonated form, where the N_δ is set to be protonated. This is also supported by the fact that N_ε should be deprotonated for the catalysis, since the enzymatic reaction would be initiated by the abstraction of the hydrogen atom of the hydroxyl group from the catalytic Ser113 by the N_ε of His358. However, we also examined the effects of the doubly protonated form of His358 as well as the singly protonated form. The resultant free energy profile and the representative structures corresponding to the metastable states of the profile revealed that the water−π coordination was not maintained in the MD simulation with ff99 (Figure 5a and 6a). This is consistent with the previous results that a water molecule cannot replace the Na^+ in the active site of T1 lipase.

MD Simulation Using ff02. We next examined the MD simulations using ff02, where His358 was set to the singly or doubly protonated form. These simulations revealed that the experimental configuration is also unstable in the presence of the water−π interaction, leading to a similar structural disruption to that of the MD simulations using ff99 (Figures 3b, 4b, 5b, and 6b). Note that this water molecule hydrogen-bonds with the Ser and His residues (Figure 1); therefore, it is possible that even in the MD simulations using ff99 and ff02, this water−π interaction is stabilized through those hydrogen bonds. Moreover, the interaction energies of ff99 and ff02 are larger than that of MP2. Nevertheless, this possibility was rejected in the present study, suggesting that the correct description of the interaction between the spherical electron density and the aromatic ring of Phe16 is essential to maintaining the structure of the catalytic site of T1 lipase.

Previous studies indicated that the contribution of the dispersion and electrostatic energies is most important for the description of the water−π interaction.[32,34,35] In fact, when the parameters describing the polarization effect in ff02 are increased, the potential curve generated by ff02 did not match that of MP2 for $r \sim 0$, although it could be fitted for $r \gg 0$ (Figure 2b). This is consistent with the results of the previous studies. On the other hand, when the parameters are decreased, the potential curve obtained by ff02 converges to that of ff99, as shown in Figure 2b. Thus, we could not find the parameters that allowed the potential curve obtained by ff02 to completely match that of MP2; therefore, ff02 cannot reproduce the MP2 result. In this manner, the failure of ff02 is derived from an incorrect description of the dispersion energy. Various attempts to improve such problems found in the force fields have been reported.[6,36−41]

Thus, the water−π coordination in T1 lipase is not possible in the MD simulations using the conventional force fields (the reasons for the structural changes are further discussed later).

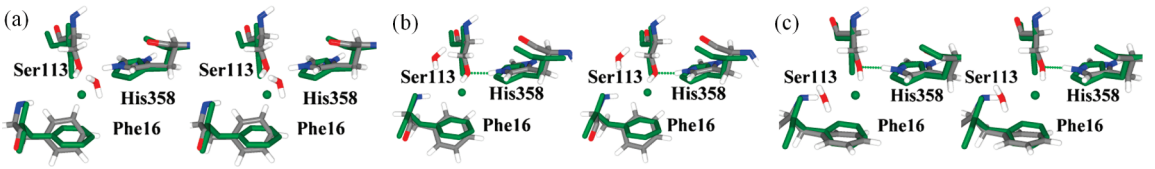

Figure 6. Conformations of the most stable state in Figure 5a (a), Figure 5b (b), and Figure 5c (c). The crystal structure of the *Geobacillus zalihae* lipase is colored green, and the snapshots of the MD simulations are shown in atom-specific colors.

In the present study, we applied our general scheme, which may be applicable to correctly reproduce any potentials using effective functions, without detailed analyses of the defects of the potential terms in the total energy functions, as described below.

MD Simulation Involving the Grid-Based Energy Representation for the $Na^+-\pi$ Interaction. As in the case of our previous study, the structural disruptions could be caused by the differences in the potential curves provided by ff99 and ff02 from the correct potential function. Accordingly, we applied our grid-based energy representation scheme to obtain the effective potential that reproduces the potential energy curve at the level of MP2. In Figure 2b and c, the potentials generated by the grid-based energy representation show that the reference energy curves (obtained by the MP2) can be reproduced for both configurations of the water−benzene complex. Then, using the optimized parameter set, we performed MD simulations of T1 lipase, in which His358 was singly or doubly protonated. The resultant 2-D free energy profiles showed that the experimental configuration was not preserved in either case, as in the results of the MD simulations using the conventional force fields (Figure 3c, 5c, and 6c).

It should be noted here that, to evaluate the stability of the conformation involving the doubly protonated His358, we required 10 ns MD simulations for the structural convergence (Figure 5c; see Supporting Information in detail). Correspondingly, for the comparison, we also extended the MD simulation where Na^+ is assigned to the spherical electron density of the catalytic site, up to 10 ns in this study. The resultant free energy profile is well converged and thus unambiguously shows consistency with the experimental data (Figure 5d). Thus, the presence of Na^+ rather than water is confirmed again.

The structural transitions observed in the present MD simulations can be understood by comparison with our previous results: In our previous MD simulation involving the grid-based energy representation for the Na^+−Phe16 interaction, both distances concerning Na^+-N_ε and Na^+−Phe16 were consistent with the experimental values, thus preserving the experimental conformation of the catalytic core of T1 lipase.[21] This would be accomplished by the strong interaction between Na^+ and the N_ε of His358. In contrast, in the present MD simulations, the interaction between the water molecule and the N_ε of His358 is not as strong as the Na^+-N_ε interaction, and so it competes for interactions with the Ser113 and His358 side chains. Namely, the weaker interaction between the water and His358 would cause the disruption, as observed in the present MD simulations using the ff99 and ff02 force fields. Conversely, this indicates that strong coordination with the surrounding amino acid residues is required to maintain the experimental structure of the catalytic core of T1 lipase, supporting the presence of Na^+, rather than water, in the catalytic site.

Thus, we have concluded that the possible presence of a water molecule, instead of Na^+, in the active site can be ruled out. Moreover, the results of our previous and present theoretical studies demonstrated that the core structure of the catalytic site of T1 lipase in the free state stably exists only in the MD simulation where Na^+ is assigned to the spherical electron density, using the correct potential fields. This further suggests that the Na^+−Phe interaction is essential for the formation of the stable core structure of the catalytic site through the formation of "Na^+ bridges", which establish the packing of the hydrophobic aromatic ring (Phe16) and the hydrophilic amino acid residues (Ser113 and His358).[24]

In the crystallographic data of biological macromolecules, similar spherical electron densities to that of the $Na^+-\pi$ complex found in T1 lipase have been widely observed. Therefore, this may be a general issue in protein science. In the present study, we have indicated that MD simulation coupled with our scheme is useful in defining the spherical electron densities, i.e., cation, water, et cetera.

CONCLUSION

In the present study, using our grid-based energy representation, we have confirmed that the core structure of T1 lipase is established by a $Na^+-\pi$ interaction, rather than a water−π interaction. In addition to the large enthalpy gain of the $Na^+-\pi$ interaction, the strong coordination of Na^+ and N_ε of His358 was also shown to be substantial to preserve the core structure of the catalytic site. Since the cation−π interactions have been widely found in biological systems, the present study will be a solid platform to further investigate crucial roles of cation−π interactions involved also in other biological systems.

The grid-based energy representation scheme can be widely applied to perform long-time MD simulations in which accurate interaction energies must be calculated at advanced post-HF method levels, with reasonable computational costs, thereby enabling us to understand the dynamic properties and functional roles of those interactions in biological macromolecules.

MATERIALS AND METHODS

Grid-Based Energy Representation. The details of the grid-based energy representation are described in the Supporting Information.[24] The outline of the scheme is as follows. The first step is to calculate a density distribution function, $\rho(\mathbf{r})$, for the grid space defined by the coordinates of a π molecule (in this work, benzene was used), using a parameter set that regulates the shape of $\rho(\mathbf{r})$. The second step is to calculate the electrostatic energy, using an effective potential that includes $\rho(\mathbf{r})$ with respect to several configurations of the water−π complex. The third step is to calculate the interaction energy between the water and the π molecule for each configuration of the complex using the total energy function, in which the original electrostatic energy term is replaced with the ρ-containing energy term. The last step is to evaluate the obtained interaction energy values by calculating their deviations from the energy values obtained from higher-level *ab initio* calculations performed beforehand. For the MD simulations using this scheme, we employed the parameter set that provided the lowest value of the deviation. The formulations of the functions used in the first, second, and third steps correspond to eqs 1, 2, and 5 in the Supporting Information, respectively.

Quantum Mechanical Calculations. All *ab initio* molecular orbital calculations of the water−benzene system were performed using Gaussian 03.[42] Geometry optimization for the isolated benzene was performed at the B3LYP[43,44]/6-311+G(d,p) level, and the optimized structure was used to construct water−benzene complex structures. For single point calculations of those structures to obtain the reference potential energy curve, we employed the Møller−Plesset second order perturbation (MP2) method[45] with an aug-cc-pvtz basis set.[46] The basis set superposition error (BSSE) was corrected by the counterpoise method.

Molecular Dynamics Calculations. All calculations were performed using the AMBER 9 program package.[47] The MD simulation of the solvated system was performed under a constant pressure of 1.013×10^5 Pa, with a periodic boundary condition at 300 K. Temperature and pressure were controlled by the Berendsen algorithm.[48] The SHAKE algorithm was used to treat the bonds involving hydrogen,[49] and the time step for integration was set to 1 fs. Electrostatic interactions were calculated by the particle mesh Ewald (PME) method,[50] with a dielectric constant of 1.0. A cutoff of 12 Å was used to calculate the direct space sum for PME.

Initial coordinates of the protein were obtained from the crystal structure of T1 lipase (Protein Data Bank accession code 2DSN[21]), but the Na^+ in the active site was replaced with a water molecule. First, hydrogen atoms were added to the crystal structure, using the LEAP module implemented in AMBER 9. The positions of the added hydrogen atoms were optimized by the steepest descent method, and then the optimization was performed for all protein atoms. The protein was subsequently immersed in a box of water molecules, consisting of 48 561 atoms modeled by TIP3P.[51] Two Na^+ ions were added to neutralize the system. Thus, the total atom number of the solvated protein system was 54 538. To relax the configuration of the solvent water molecules, the MD simulation was performed for 10 ps at 300 K, where a harmonic constraint was applied to all protein and Na^+ atoms with a force constant of 500 kcal mol^{-1} $Å^{-2}$. With respect to the density distribution function, the optimized values of a_x, a_y, and a_z for the carbon atoms were 0.198, 0.198, and 0.337 Å, respectively, and those for the hydrogen atoms were 0.225, 0.225, and 0.312 Å, respectively. The value of α in the cutoff function was set to 1.0×10^{-5}. A cube, with its center located on the center of mass of the aromatic ring, was generated; the volume of the cube was 10^3 $Å^3$, and the grid-point space inside the cube was set to 0.2 Å. Accordingly, the number of grid points involved in the cube was 125 000.

■ ASSOCIATED CONTENT

Supporting Information. Further descriptions concerning the grid-based energy representation and the examination of the doubly protonated form of His358 are available. This material is available free of charge via the Internet at http://pubs.acs.org.

■ AUTHOR INFORMATION

Corresponding Author

*Tel.: (+81)-791-58-0347. Fax: (+81)-791-58-0347. E-mail: tateno@sci.u-hyogo.ac.jp.

■ ACKNOWLEDGMENT

This work was partly supported by Grants-in-Aid from the Ministry of Education, Culture, Sports, Science and Technology (MEXT), under contract Nos. 21340108 and 23654120. Computations were performed using the computer facilities under the "Interdisciplinary Computational Science Program" at the Center for Computational Sciences, University of Tsukuba, the Computer Center for Agriculture, Forestry, and Fisheries Research, MAFF, Japan, and the Supercomputer Center, Institute for Solid State Physics, University of Tokyo. J.K. was supported by a Research Fellowship of the Japan Society for the Promotion of Science.

■ REFERENCES

(1) Chan, D. I.; Prenner, E. J.; Vogel, H. J. *Biochim. Biophys. Acta* **2006**, *1758*, 1184–1202.
(2) Dougherty, D. A. *Science* **1996**, *271*, 163–168.
(3) Dougherty, D. A. *J. Nutr.* **2007**, *137*, 1504S–1508S.
(4) Gallivan, J. P.; Dougherty, D. A. *Proc. Natl. Acad. Sci. U.S.A.* **1999**, *96*, 9459–9464.
(5) Ma, J. C.; Dougherty, D. A. *Chem. Rev.* **1997**, *97*, 1303–1324.
(6) Minoux, H.; Chipot, C. *J. Am. Chem. Soc.* **1999**, *121*, 10366–10372.
(7) Dunbar, R. C. *J. Phys. Chem. A* **2000**, *104*, 8067–8074.
(8) Gapeev, A.; Dunbar, R. C. *J. Am. Chem. Soc.* **2001**, *123*, 8360–8365.
(9) Kish, M. M.; Ohanessian, G.; Wesdemiotis, C. *Int. J. Mass Spectrom.* **2003**, *227*, 509–524.
(10) Ruan, C. H.; Rodgers, M. T. *J. Am. Chem. Soc.* **2004**, *126*, 14600–14610.
(11) Ryzhov, V.; Dunbar, R. C.; Cerda, B.; Wesdemiotis, C. *J. Am. Soc. Mass Spectrom.* **2000**, *11*, 1037–1046.
(12) Siu, F. M.; Ma, N. L.; Tsang, C. W. *J. Am. Chem. Soc.* **2001**, *123*, 3397–3398.
(13) Costanzo, F.; Della Valle, R. G. *J. Phys. Chem. B* **2008**, *112*, 12783–12789.
(14) Hu, J.; Barbour, L. J.; Gokel, G. W. *Proc. Natl. Acad. Sci. U.S.A.* **2002**, *99*, 5121–5126.
(15) Meadows, E. S.; De Wall, S. L.; Barbour, L. J.; Gokel, G. W. *J. Am. Chem. Soc.* **2001**, *123*, 3092–3107.
(16) Kooystra, P. J.; Kalk, K. H.; Hol, W. G. *Eur. J. Biochem.* **1988**, *177*, 345–349.
(17) Labesse, G.; Ferrari, D.; Chen, Z. W.; Rossi, G. L.; Kuusk, V.; McIntire, W. S.; Mathews, F. S. *J. Biol. Chem.* **1998**, *273*, 25703–25712.
(18) Liaw, S. H.; Kuo, I.; Eisenberg, D. *Protein Sci.* **1995**, *4*, 2358–2365.
(19) Wouters, J. *Protein Sci.* **1998**, *7*, 2472–2475.
(20) Wouters, J.; Maes, D. *Acta Crystallogr., Sect. D: Biol. Crystallogr.* **2000**, *56*, 1201–1203.
(21) Matsumura, H.; Yamamoto, T.; Leow, T. C.; Mori, T.; Salleh, A. B.; Basri, M.; Inoue, T.; Kai, Y.; Rahman, R. N. *Proteins* **2008**, *70*, 592–598.
(22) Fischer, M.; Pleiss, J. *Nucleic Acids Res.* **2003**, *31*, 319–321.
(23) Steiner, T. *Biophys. Chem.* **2002**, *95*, 195–201.
(24) Hagiwara, Y.; Matsumura, H.; Tateno, M. *J. Am. Chem. Soc.* **2009**, *131*, 16697–16705.
(25) Cheatham, T. E., III; Cieplak, P.; Kollman, P. A. *J. Biomol. Struct. Dyn.* **1999**, *16*, 845–862.
(26) Ran, J.; Hobza, P. *J. Chem. Theory Comput* **2009**, *5*, 1180–1185.
(27) Cieplak, P.; Caldwell, J.; Kollman, P. *J. Comput. Chem.* **2001**, *22*, 1048–1057.
(28) Jurecka, P.; Sponer, J.; Cerny, J.; Hobza, P. *Phys. Chem. Chem. Phys.* **2006**, *8*, 1985–1993.
(29) Tsuzuki, S.; Honda, K.; Uchimaru, T.; Mikami, M.; Tanabe, K. *J. Am. Chem. Soc.* **2002**, *124*, 104–112.
(30) Jain, A.; Ramanathan, V.; Sankararamakrishnan, R. *Protein Sci.* **2009**, *18*, 595–605.
(31) Li, S.; Cooper, V. R.; Thonhauser, T.; Puzder, A.; Langreth, D. C. *J. Phys. Chem. A* **2008**, *112*, 9031–9036.
(32) Mishra, B. K.; Sathyamurthy, N. *J. Phys. Chem. A* **2007**, *111*, 2139–2147.
(33) Bas, D. C.; Rogers, D. M.; Jensen, J. H. *Proteins* **2008**, *73*, 765–783.
(34) Tsuzuki, S.; Honda, K.; Uchimaru, T.; Mikami, M.; Tanabe, K. *J. Am. Chem. Soc.* **2000**, *122*, 11450–11458.
(35) Riley, K. E.; Pitoňák, M.; Černý, J. i.; Hobza, P. *J. Chem. Theory Comput* **2010**, *6*, 66–80.
(36) Soteras, I.; Orozco, M.; Luque, F. J. *Phys. Chem. Chem. Phys.* **2008**, *10*, 2616–2624.
(37) Chipot, C.; Maigret, B.; Pearlman, D. A.; Kollman, P. A. *J. Am. Chem. Soc.* **1996**, *118*, 2998–3005.

(38) Cubero, E.; Luque, F. J.; Orozco, M. *Proc. Natl. Acad. Sci. U.S.A.* **1998**, *95*, 5976–5980.
(39) Wormer, P. E. S.; van der Avoird, A. *Chem. Rev.* **2000**, *100*, 4109–4144.
(40) Mishra, B. K.; Sathyamurthy, N. *J. Phys. Chem. A* **2007**, *111*, 2139–2147.
(41) Salonen, L. M.; Ellermann, M.; Diederich, F. *Angew. Chem., Int. Ed.* **2011**, *50*, 4808–4842.
(42) Frisch, M. J. *Chem. Listy* **2006**, *100*, A9–A9.
(43) Becke, A. D. *J. Chem. Phys.* **1993**, *98*, 5648–5652.
(44) Lee, C. T.; Yang, W. T.; Parr, R. G. *Phys. Rev. B* **1988**, *37*, 785–789.
(45) Headgordon, M.; Pople, J. A.; Frisch, M. J. *Chem. Phys. Lett.* **1988**, *153*, 503–506.
(46) Dunning, T. H. *J. Chem. Phys.* **1989**, *90*, 1007–1023.
(47) Case, D. A.; Cheatham, T. E.; Darden, T.; Gohlke, H.; Luo, R.; Merz, K. M.; Onufriev, A.; Simmerling, C.; Wang, B.; Woods, R. J. *J. Comput. Chem.* **2005**, *26*, 1668–1688.
(48) Berendsen, H. J. C.; Postma, J. P. M.; Vangunsteren, W. F.; Dinola, A.; Haak, J. R. *J. Chem. Phys.* **1984**, *81*, 3684–3690.
(49) Ryckaert, J. P.; Ciccotti, G.; Berendsen, H. J. C. *J. Comput. Phys.* **1977**, *23*, 327–341.
(50) Darden, T.; York, D.; Pedersen, L. *J. Chem. Phys.* **1993**, *98*, 10089–10092.
(51) Jorgensen, W. L.; Madura, J. D. *J. Am. Chem. Soc.* **1983**, *105*, 1407–1413.